Ligand-Bridged Oligomeric and Supramolecular Arrays of the Hexanuclear Rhenium Selenide Clusters—Exploratory Synthesis, Structural Characterization, and Property Investigation†

HUGH D. SELBY, BRYAN K. ROLAND, AND ZHIPING ZHENG*

Department of Chemistry, University of Arizona, Tucson, Arizona 85721

Received June 6, 2003

ABSTRACT

Transition metal clusters, by virtue of their well-defined structures and unique properties, present themselves as an attractive class of structural and functional building blocks for molecular and supramolecular construction. Summarized in this Account are highlights of our efforts utilizing face-capped octahedral $[Re_6(\mu_3\text{-}Se)_8]^{2+}$ clusters as the fundamental building units to create a wide variety of preprogrammed architectures. These include molecular "Tinkertoys", featuring stereospecific cluster units bridged by multitopic ligands and extended arrays of clusters engineered via hydrogen bonding and secondary metal−ligand coordination.

I. Introduction

The goal of controlling matter on the scale of individual molecules and, more recently, atoms has captured the imagination of scientists.[1] The primary impetus is the prospect of creating molecular or supramolecular assemblies that are capable of performing sophisticated physicochemical functions. Although the applications of such assemblies remain largely in the realm of speculation, great progress has been made in the development of various constructing elements. Most notable in this context has been the use of transition metals in conjunction with polydentate ligands, leading to numerous preprogrammed architectures, many of which not only are of consummate structural beauty but also display interesting and potentially useful properties.[2]

We envision an analogous yet probably more intriguing chemistry wherein polynuclear clusters surrogate for single metal ions. From a structural viewpoint, the multiple metal sites available in a cluster allow for site differentiation, that is, selective binding to purpose-specific ligands. Thus, a range of building blocks with systematically varied and rigidly fixed stereochemistries may be realized. The fixed stereochemistries impart the shape and directionality critical to the desired assemblies. From the perspective of achieving functional materials, metal clusters are unique and attractive because they frequently exhibit interesting traits that are inherent to metal−metal bonded species.[3] The efforts to build cluster-supported molecular or supramolecular structures are thus expected to offer many fascinating research problems with potentially significant ramifications.

A number of groups have investigated the use of metal clusters for the construction of molecular or more extended supramolecular arrays. For example, Yaghi and co-workers have created porous metal−organic frameworks supported by octahedral zinc carboxylate clusters for hydrogen storage.[4] Using a trinuclear zinc cluster complex with an enantiopure carboxylate ligand, Kim and co-workers have prepared homochiral porous materials for enantioselective separation and catalysis.[5] More recently, Cotton and co-workers have elaborated supramolecular constructions using metal−metal bonded dimeric clusters as building blocks.[6] In a similar capacity, Shriver and co-workers have applied hexanuclear clusters containing the $[Mo_6(\mu_3\text{-}Cl)_8]^{4+}$ core, together with bridging 4,4′-dipyridyl ligands, for the preparation of microporous xerogels that are capable of size-selective ion exchange.[7] Utilizing an octahedral tungsten cluster anion $[W_6(\mu_3\text{-}S)_8(CN)_6]^{6-}$ as a building block, three-dimensional extended coordination networks with transition metal ions M^{2+} (M = Mn, Fe, Co, Zn) have recently been obtained.[8]

Stimulated by these previous efforts and by the potential materials applications of metal chalcogenide clusters,[9] we embarked on a tour of constructing oligomeric and polymeric arrays by employing hexarhenium chalcogenide clusters featuring the $[Re_6(\mu_3\text{-}Q)_8]^{2+}$ (Q = S, Se, Te) core[10] as building blocks. In this Account, highlights of our efforts are summarized.

II. Hexarhenium Chalcogenide Clusters—A Class of Versatile Building Blocks

Soluble molecular clusters of the hexarhenium chalcogenides are a rather recent development in cluster chemistry.[10] The 24-electron, face-capped hexanuclear core, shown in Figure 1, can be viewed as an octahedron of rhenium atoms enclosed in a cube formed by substitutionally inert chalcogenide ligands. Halide-terminated clusters of the general formula $[Re_6(\mu_3\text{-}Q)_8X_6]^{4-}$ (X = Cl,

Hugh D. Selby received his B.S. degree in 1997 from the University of New Mexico. He came to the University of Arizona in 1998, and is completing his Ph.D. thesis work with Professor Zheng on supramolecular materials of metal clusters. He received a GenCorp Fellowship for Synthetic Chemistry (2000).

Bryan K. Roland earned his B.S. degree from the College of Wooster in 1998. Soon afterward, he joined the Zheng group at the University of Arizona and has been studying cluster-supported supramolecular and hybrid materials.

Zhiping Zheng received his B.S. and M.S. degrees in chemistry from Peking University, China, and his Ph.D. from UCLA in1995 with Professor M. Frederick Hawthorne. After conducting postdoctoral research with Professor Richard H. Holm at Harvard University, he joined the faculty of the University of Arizona in 1997. His current research is focused on supramolecular chemistry and materials, which involves the elaboration of polynuclear lanthanide complexes and transition metal clusters. He received an NSF CAREER Award and an international Junior Award (2003) from the European Rare Earth and Actinide Society.

† Dedicated to Professor Richard H. Holm on the occasion of his 70th birthday.

* To whom correspondence should be addressed. Phone: (520) 626-6495. Fax: (520) 621-8407. E-mail: zhiping@u.arizona.edu.

10.1021/ar020134c CCC: $25.00
Published on Web 10/02/2003

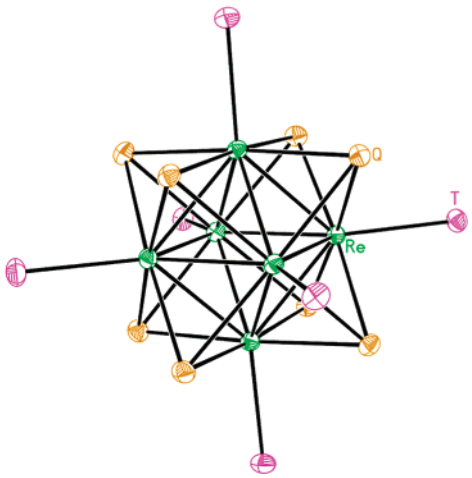

FIGURE 1. Structure of the $[Re_6(\mu_3\text{-}Q)_8]^{2+}$ cluster shown with terminal ligands (T).

Br, I; Q = S, Se) are obtained from the initial solid-state synthesis.[11] Unlike their isomorphs of the earlier transition metal halides or chalcogenides,[12] these clusters are stable to aerobic handling and vigorous synthetic conditions, yet labile enough that solution-phase transformations are easily accomplished.[13,14a] It has been found that the halide-terminated starting clusters undergo facile ligand substitution reactions with triethylphosphine to yield site-differentiated complexes of the general formula $[Re_6(\mu_3\text{-}Q)_8(PEt_3)_nX_{6-n}]^{(n-4)+}$ (for Q = S, n = 2−6, X = Br^-; for Q = Se, n = 4−6, X = I^-).[13a,d] Subsequent de-halogenation in coordinating media L, often a coordinating solvent, leads to corresponding derivatives of the general formula $[Re_6(\mu_3\text{-}Q)_8(PEt_3)_nL_{6-n}]^{2+}$ with unperturbed stereochemistries.[13]

More attractive from the perspective of creating novel materials are the interesting electrochemical and photophysical properties of the clusters.[13,14] A reversible, one-electron oxidation event is typically observed for these clusters. The clusters are phosphorescent, and the phosphorescence is dependent on the coordination environment of the cluster.[14] These interesting traits, though not yet fully understood due largely to the complicated electronic structures of the cluster system, suggest the possibility of creating cluster-based functional materials.[15]

Indeed, their well-behaved chemistry and interesting electrochemical and photophysical properties have made these clusters the subject of recent intensive research. For example, the groups of Long[16] and Fedorov[17] have independently prepared cyano-bridged $[Re_6(\mu_3\text{-}Q)_8]$ cluster−metal framework solids, including cluster-expanded Prussian blue analogues by Long's group.[16a] Some of these materials display interesting host−guest chemistry that may be useful for sensory applications.[16b]

Rather than relying on a single highly symmetric building block such as $[Re_6(\mu_3\text{-}Q)_8(CN)_6]^{4-}$, we anticipate more extensive and versatile synthetic chemistry with the use of stereospecific cluster complexes featuring two different types of terminal ligands, one of which serves to protect certain metal sites while the other provides the reactive sites necessary for further transformations.[13] The cluster core's inertness prohibits stereochemical scrambling and, combined with the wide displacement of relatively rigid ligands, effectively eliminates the flexibility that frequently complicates molecular or supramolecular construction based on mononuclear and even dinuclear complexes.

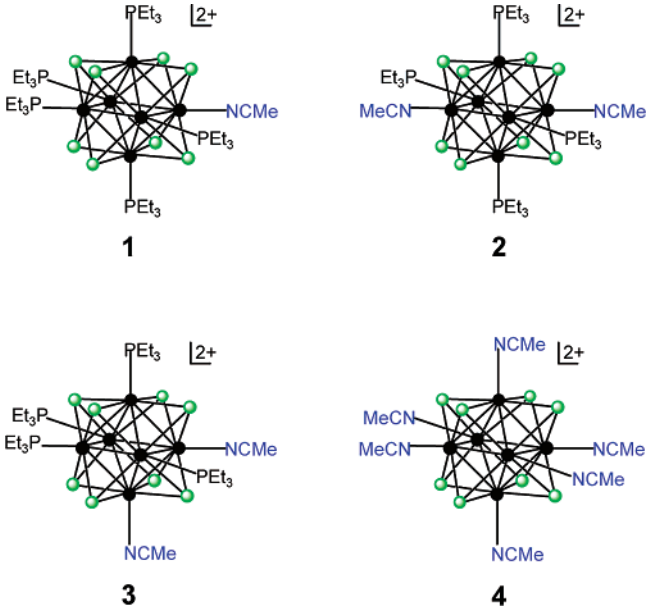

FIGURE 2. Molecular structures of isosteric acetonitrile solvates of the $[Re_6(\mu_3\text{-}Se)_8]^{2+}$ cluster.

The relevant stereospecific precursors for our synthetic efforts are the acetonitrile solvates of the general formula $[Re_6(\mu_3\text{-}Se)_8(PEt_3)_n(MeCN)_{6-n}]^{2+}$ {Figure 2; n = 5 (**1**), 4 [trans- (**2**) and cis- (**3**)], 0 (**4**)}.[13a−c] These solvates can be readily prepared by de-iodination of the corresponding $[Re_6(\mu_3\text{-}Se)_8(PEt_3)_nI_{6-n}]^{(n-4)+}$ complexes with $AgSbF_6$ in the presence of MeCN. In our investigation, these conveniently prepared solvates have acted as the geometric basis. However, their application in actual synthesis falls into two distinct methodologies. In the first approach, the solvates react with specific multitopic ligands to create arrays, wherein a number of clusters are "condensed" by the cluster-bridging ligands with concomitant expulsion of the acetonitrile molecule(s). The second method, representing something of a paradigm shift, entails solvent displacement by ligands that bear additional functional groups capable of *secondary* (with respect to *primary* cluster ligation) interactions, such as hydrogen bonding and metal−ligand coordination. In this way, multicluster arrays mediated by the secondary interactions can be fabricated. In the following sections, the successful applications of the cluster solvates in the context of these two distinct paradigms will be illustrated.

III. Molecular Tinkertoys Featuring the $[Re_6(\mu_3\text{-}Se)_8]^{2+}$ Clusters and Multitopic Ligands

Using judiciously designed molecular building blocks—the molecular version of Tinkertoys kits—a wide variety of structural and functional assemblies, instead of the fanciful windmills or whimsical vehicles of the macro-

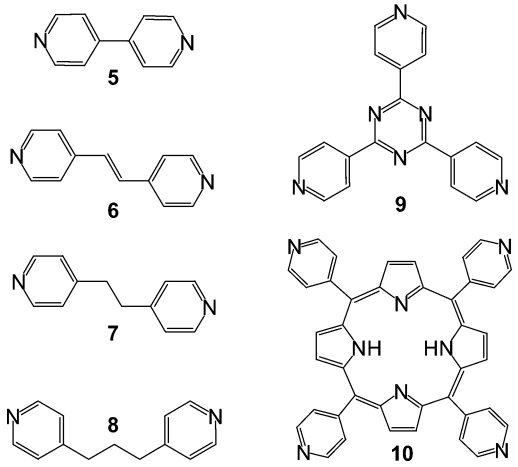

FIGURE 3. Molecular structure of multitopic ligands based on the 4-pyridyl coordinating moiety.

Scheme 1

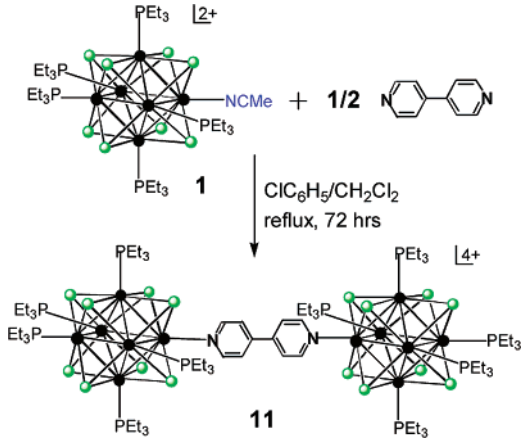

scopic toy set, can be realized. Specific isomers of the nitrile solvated clusters, differing from one another only in the number and spatial arrangement of the terminal ligands, may be viewed as the "spools" that are equipped with reactive sites instead of holes. The multitopic ligands (**5**−**10**, Figure 3), featuring a number of metal-coordinating sites arranged divergently, can be regarded as the "sticks" that introduce branches, angles, or loops to fix the desired geometry. The prototype of this assembly method entails the condensation of the nitrile solvate of the pentaphosphine-substituted cluster with a half equivalent of a bidentate ligand in refluxing chlorobenzene to give a dumbbell-shaped dicluster bridged by the ditopic ligand (**11**, Scheme 1).[13c] This methodology is readily applicable to the construction of other multicluster arrays of predetermined shapes and dimensions, including cluster-supported molecular squares,[18] star-shaped tri- and tetraclusters,[19] and dendrimers of clusters.[20]

A. Molecular Squares. The design and synthesis of squares from molecular building blocks has received much recent interest, due largely to their interesting host−guest chemistry and possible applications for recognition, binding, and activation of guest species. Relying on the intrinsic right angle of *cis*-$[Re_6(\mu_3\text{-}Se)_8(PEt_3)_4(MeCN)_2](SbF_6)_2$ (**3**) to direct the geometric outcome of the reaction

Scheme 2

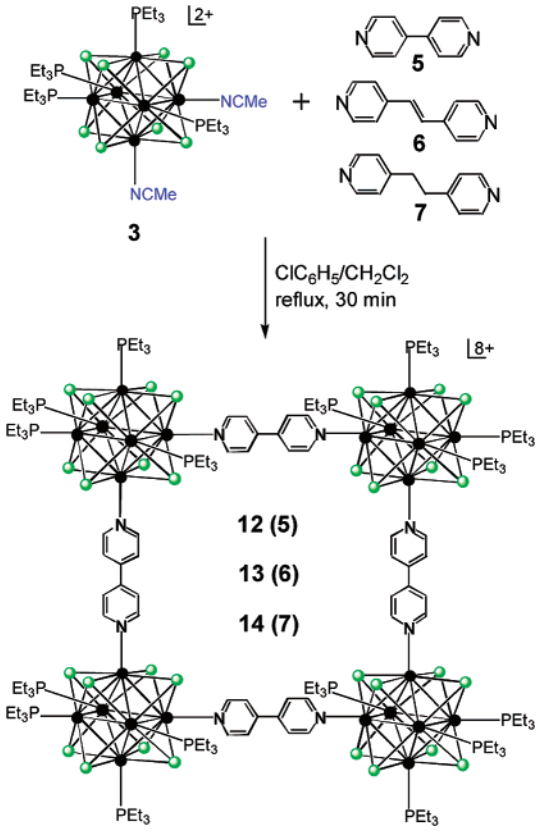

with stoichiometric equivalents of 4,4′-dipyridyl derivatives, the first examples of molecular squares supported by hexanuclear transition metal clusters have been realized (**12**−**14**, Scheme 2).[18] The structures of these square-shaped multicluster arrays were established by using spectroscopic techniques and microanalysis. These soluble, highly charged entities with nanosized pores invite examination of their potential of guest binding and activation, with an eye to possibilities in homogeneous catalysis.

B. Molecular Stars. In the bridging capacity, star-shaped connectors carrying arms at fixed angles in a plane, e.g., 120° (**9**) and 90° (**10**) in Figure 3, offer greater structural sophistication than the straightforward ditopic ligands. Indeed, utilizing the pentaphosphine-substituted nitrile solvate $[Re_6(\mu_3\text{-}Se)_8(PEt_3)_5(MeCN)](SbF_6)_2$ (**1**) and the star-shaped connectors **9** and **10** from the Tinkertoy kit, two-dimensional cluster oligomers were obtained, wherein three or four cluster units are attached to the planar scaffold (**15** and **16**, Scheme 3).[19]

The ultimate proof of the structure of the tricluster is provided by single-crystal X-ray diffraction. The ORTEP presentation (Figure 4) shows three units of $[Re_6(\mu_3\text{-}Se)_8(PEt_3)_5]^{2+}$ attached to the central tritopic ligand via coordination of the pyridyl N atoms.

Non-interaction between the clusters of **11** has previously been inferred from the observation of only a single redox wave at a potential that is essentially identical to that of a monocluster. Similar electrochemical behaviors were observed for the tri- and tetracluster arrays. Coulometry confirmed the electron counts,[21] with the overlay of the cyclic voltammograms (Figure 5) demonstrating

Scheme 3

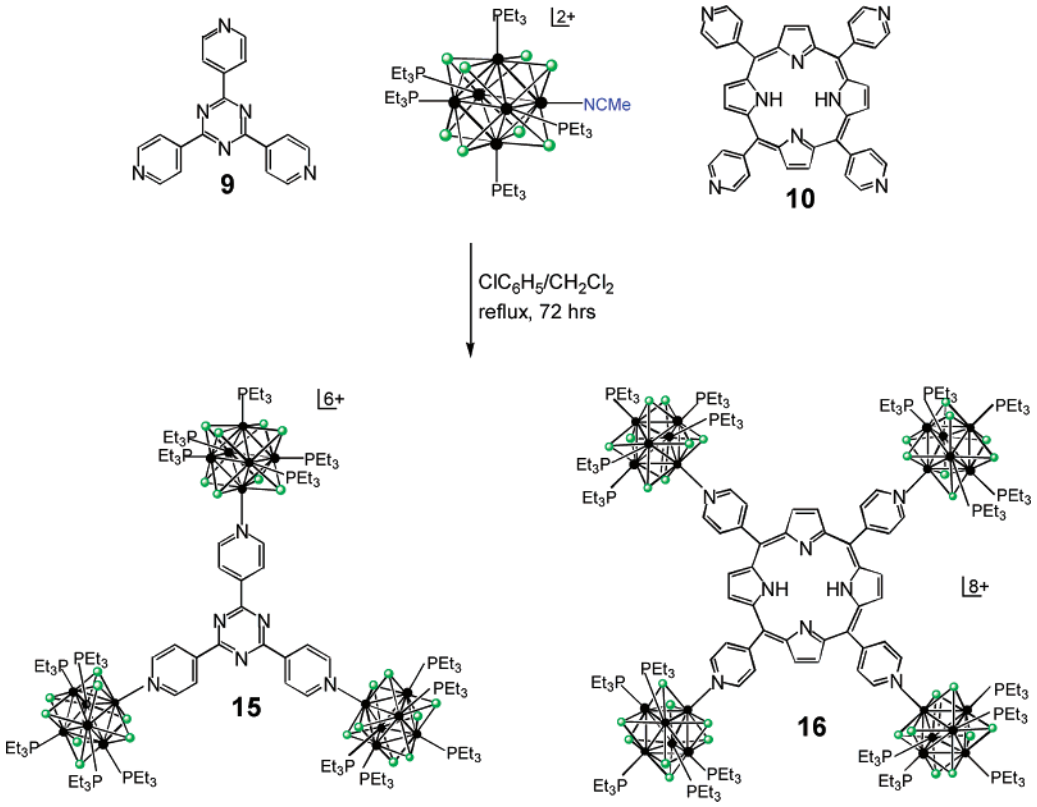

qualitatively a nice correlation between the number of clusters and the number of electrons involved in the redox event.

Interesting properties may be anticipated for these multicluster arrays. For example, compound **15**, possessing a three-fold rotational symmetry (octupolar chromophores), may display two-photon absorption properties as well as improved second-order nonlinear optical properties.[22] Metal (divalent Co, Ni, Cu, and Zn) complexes of the cluster-studded tetrapyridylporphyrin **16** are expected to exhibit rich electrochemistry and catalytic properties, analogous to what has been demonstrated for the well-studied polyruthenated species.[23]

C. Molecular Trees. Dendrimers are a class of hyperbranched synthetic polymers emanating from a central core. A great variety of metallodendrimers have been prepared by utilizing transition metal ions in conjunction with polydendate ligands, whereby the metal−ligand dative bond serves to drive and direct the assembly of dendrimers.[24] We envision an analogous chemistry wherein the $[Re_6(\mu_3\text{-}Se)_8]^{2+}$ clusters serve as structural and functional scaffolds for dendrimer construction. Synthetically, one-pot ligand substitution reaction of the fully solvated hexanuclear cluster may lead to the addition of six

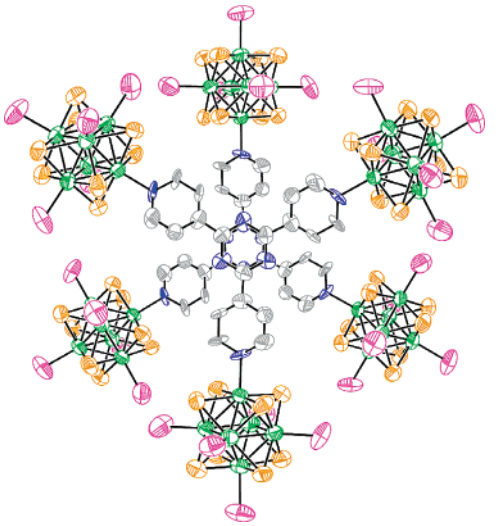

FIGURE 4. ORTEP view (50% ellipsoids) showing two units of the cationic core of **15**, with a separation of 11.27 Å between the central aromatic rings, in a staggered disposition. Ethyl groups are omitted for clarity. Color scheme: C, gray; N, blue; P, purple; Re, green; Se, brown.

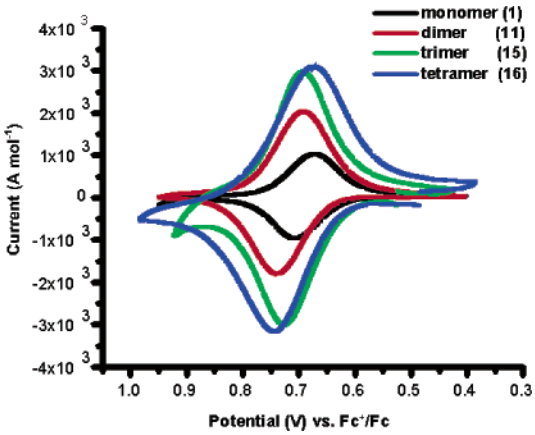

FIGURE 5. Overlay of cyclic voltammograms of monocluster **1** and three oligomeric clusters-of-clusters (**11**, **15**, **16**).

Scheme 4

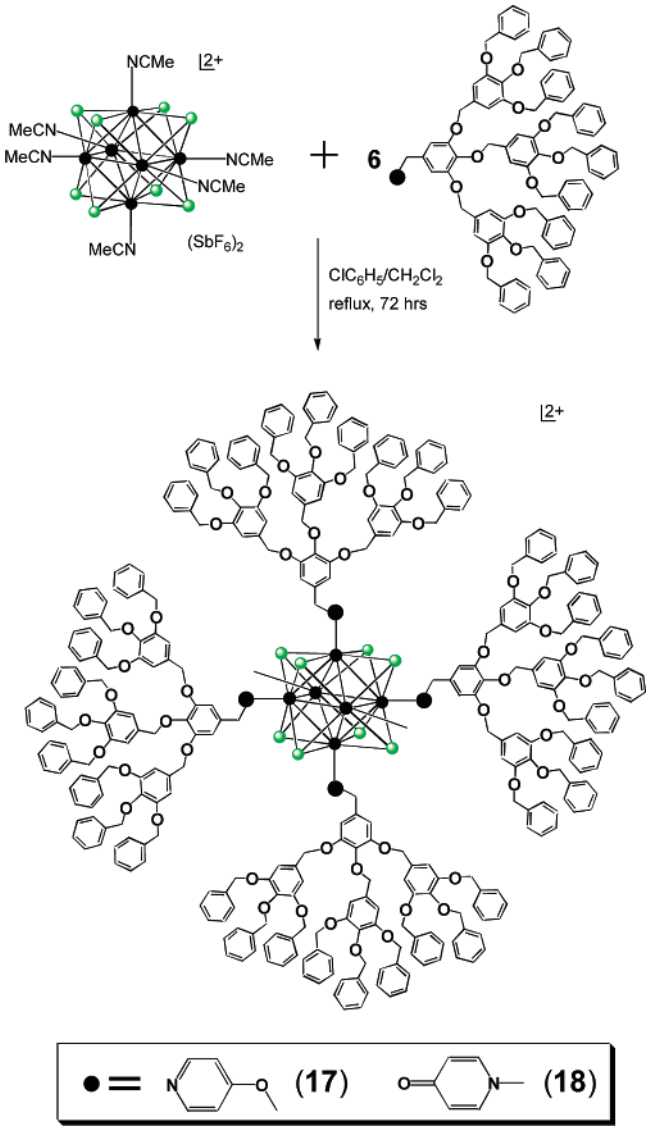

dendron ligands, yielding a globular system even with low-generation dendrons. The octahedral disposal of six metal sites establishes a very open arrangement of the dendrons, thus reducing possible structural defects due to steric congestion at higher dendritic generations. Functionally, the redox-active and photoactive clusters would be ideal for the integration of interesting properties within the nanoscopic dimensions of a dendrimer. Finally, because dendrimer synthesis is modular, one could selectively modify the dendrons prior to linking them to the core. Thus, extremely precise control of the dendrimer's properties is possible.

Our efforts in this vein have resulted in the first metallodendrimers centered on the $[Re_6(\mu_3\text{-}Se)_8]^{2+}$ core (**17** and **18**, Scheme 4; only four of the six dendrons are shown for clarity).[20a] These novel metallodendrimers exhibit intriguing photophysical properties that are profoundly affected by the dendritic ligands (Figure 6). A pyridyl-based dendron leads to the formation of the cluster-cored metallodendrimer **17**, whose electronic absorption does not differ significantly from that of the parent cluster **4**.

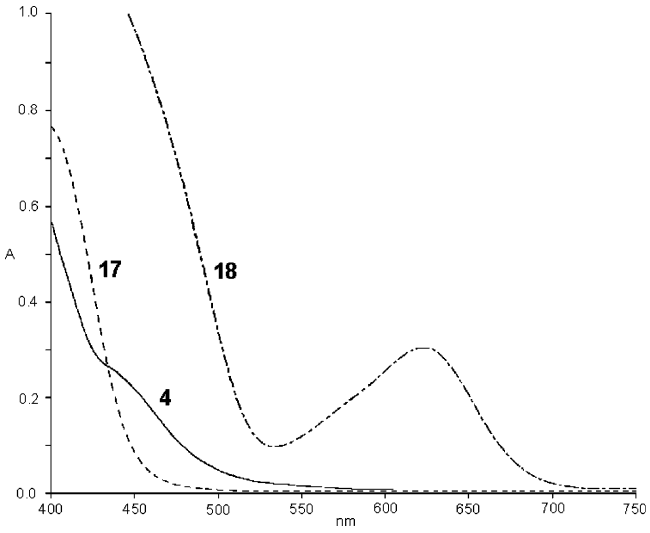

FIGURE 6. Electronic spectra of **4**, **17**, and **18** in CH_2Cl_2 solutions.

In stark contrast, dendrimer **18**, formed with pyridone-based dendrons, displays a dramatic color change to emerald green from the orange-red of the starting cluster. We note that this color change is similar to that observed during the exhaustive oxidation of monocluster **1** (Figure 2) and the bridged dicluster **11** (Scheme 1). Furthermore, the electronic absorption of **18**, shown in Figure 6, resembles closely that of the oxidized cluster species $[Re_6(\mu_3\text{-}Se)_8I_6]^{3-}$.[11,13c] All taken into consideration, it seems reasonable to believe that a shift in oxidation potential of the cluster occurs when the new pyridone-based dendrons are attached, causing spontaneous oxidation to the $[Re_6(\mu_3\text{-}Se)_8]^{3+}$ cluster in solution. The electrochemistry of these cluster-supported dendrimers is currently under investigation.

Bona fide cluster dendrimers, characterized by the presence of cluster building blocks at the core, within the branching units, and on the periphery of the dendrimer, are not yet known. Such species may have interesting properties related to both the component clusters and the unique molecular arrangement of the cluster building blocks. Keen to explore this notion, we have prepared the prototype of dendritic multicluster arrays—three first-generation metallodendrimers, each featuring a central $[Re_6(\mu_3\text{-}Se)_8]^{2+}$ core surrounded by six units of $[Re_6(\mu_3\text{-}Se)_8(PEt_3)_5L]^{2+}$ (L = a ditopic ligand); the dipyridyl-based ligands bridge the central and the peripheral clusters.[20b]

The synthesis of the heptacluster dendrimers is set out in Scheme 5. Tinkertoy-type ligand exchange of $[Re_6(\mu_3\text{-}Se)_8(PEt_3)_5(MeCN)](SbF_6)_2$ (**1**) with an excess of bidentate ligands produced the site-differentiated cluster dendrons, $[Re_6(\mu_3\text{-}Se)_8(PEt_3)_5L](SbF_6)_2$ [**19** (L = **6**), **20** (L = **7**), **21** (L = **8**)], bearing an accessible pyridyl N atom capable of further metal coordination. Subsequent reactions of the dendrons with the fully solvated cluster complex **4** afforded the targeted dendrimers, **22**−**24**. In addition to the usual characterization by ^1H and ^{31}P NMR studies, the most convincing evidence supporting the proposed dendritic architecture came from comparative ^{77}Se NMR studies of **4**, the dendrons, and the resulting dendrimers.

Scheme 5

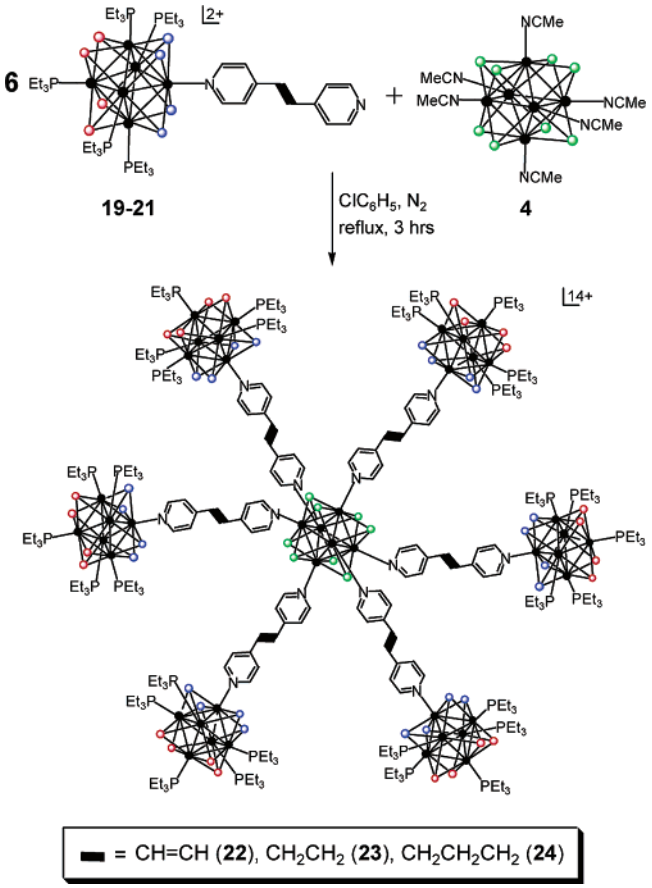

The representative study concerning **23** is shown in Figure 7. As suggested by the top spectrum, the Se atoms of **23** are present in three distinct chemical environments, which are indicated in different colors in Scheme 5. The relative signal intensity indicates a ratio of 3:3:1 for the different types of Se; such a ratio is mandated by, and thus in agreement with, the formulation of the hepta-cluster dendrimer. The signal at −249 ppm is a new feature when the spectrum is compared with that of dendron **20**, and is ascribed to the Se atoms associated with the central cluster core. This resonance is shifted downfield by 35 ppm from its equivalent at −284 ppm of parent **4**. The ^{77}Se resonances of the peripheral clusters remain essentially unchanged, likely because the local structural alteration upon dendrimer formation is minimal. This technique is especially valuable when X-ray-quality single crystals are unavailable or the product identity cannot be unambiguously established by other characterization means, such as mass spectrometry.

Cyclic voltammetric experiments of **22** reveal two oxidation events, the first at $E_{1/2}$ = 0.73 V (vs the ferrocenium/ferrocene redox couple) and chemically reversible, and the second at 0.88 V but not as well-defined as the first process. The ratio of 6:1 of the number of electrons involved suggests that the first oxidation originates from the peripheral clusters, while the oxidation at the higher potential is due to the oxidation of the central cluster. Intercluster electronic coupling is apparent, as the one-electron oxidation of various cluster complexes at

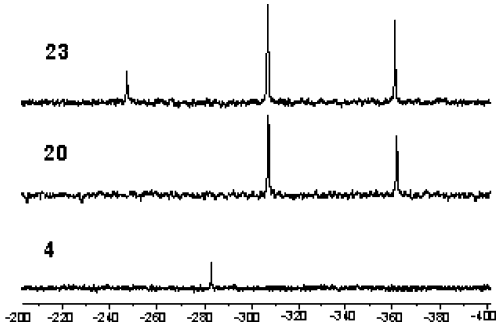

FIGURE 7. ^{77}Se NMR spectra of **4**, **20**, and **23**.

almost identical potentials should otherwise occur, as previously demonstrated.[13c] This rare observation of intercluster interactions may be understood in terms of charge buildup within this compact and highly charged dendritic architecture as well as possible electron delocalization. The only other report of intercluster electronic coupling is in the dicluster *trans*-{$[Re_6(\mu_3\text{-}Se)_8(PEt_3)_4]_2(MeCN)_2$}$^{4+}$, where the two component clusters are in intimate contact via rhombic Re−Se bridges; two coupled oxidations separated by 0.25 V are observed.[13b]

IV. Cluster Arrays Mediated by Secondary Interactions of Purpose-Specific Ligands

As we have seen, a variety of ligand-bridged oligomeric clusters can be constructed by interlinking stereospecific cluster units with appropriate multitopic ligands. However, the conditions are quite forcing, suggesting that a concerted condensation or rapid cyclization must occur. It is entirely possible that a slight change in conditions might favor uncontrolled polymerization over the cyclization/condensation reaction. Indeed, an attempt to form a molecular cube using *fac*-$[Re_6(\mu_3\text{-}Se)_8(PPh_3)_3(MeCN)_3](SbF_6)_2$[21] and 4,4′-dipyridyl via the Tinkertoy-condensation route afforded a completely intractable solid. Thus, in terms of preparing porous materials of higher dimension or extent, the condensation reaction is likely limited in scope. An additional problem arises upon consideration of the identity of the final products. Although the stereochemistry and molecular structure of these novel assemblies can be established by spectroscopic means, structural determination is often difficult or impossible due to the lack of single crystals suitable for X-ray diffraction. The high charges, the presence of many easily disordered counterions, and the fairly open structures in the case of porous assemblies all presumably contribute to this difficulty. Consequently, structure−property correlation of these materials is often challenging.

Faced with such synthetic difficulties, and seeking to overcome the challenges of crystallization, we have invoked the second synthetic paradigm—cluster-directed self-assembly via two distinct *secondary* interactions of purpose-specific ligands. In the first (Figure 8a), a rhenium cluster complex is formed with at least one ligand L (isonicotinamide, for example) that bears functionality capable of intermolecular hydrogen bonding. Supra-

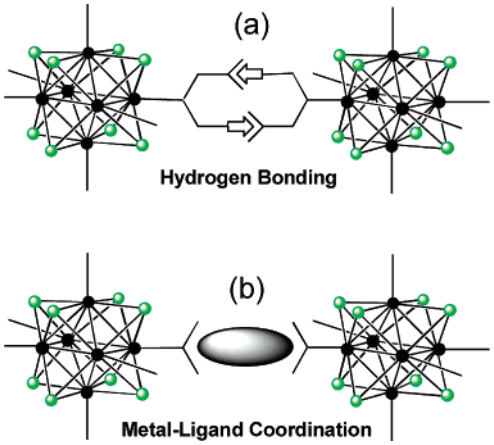

FIGURE 8. Schematic demonstration of hydrogen bonding (a) and metal−ligand coordination (b) interactions for mediating the assembly of multicluster arrays.

molecular cluster arrays can then be produced by virtue of the intercluster hydrogen bonds. In the second (Figure 8b), a cluster complex equipped with a ligand (4,4′-dipyridyl, for instance) that possesses a free coordinating atom is used as a cluster-derived ligand for secondary metal coordination. Multicluster arrays can thus be assembled via secondary coordination to the single metal ions. This latter approach is in line with the well-established "complex-as-ligand" methodology,[25] but using a much bulkier cluster motif in place of a single metal ion. Both approaches maintain the ease of handling offered by the monocluster species in solution yet offer the possibility of obtaining crystalline samples, frequently in the form of single crystals, of the extended arrays when assembled in the solid state.

A. Multicluster Arrays Assembled via Intercluster Hydrogen Bonding. By using the site-differentiated cluster complexes as the hydrogen-bonding basis, geometric and dimensional control of the cluster is added to the directionality of the hydrogen bond. Ideally, the additional structural handle would provide an extra degree of control of the self-assembly process. To this end, a series of site-differentiated cluster complexes of the general formula $[Re_6(\mu_3\text{-}Se)_8(PEt_3)_n(\text{isonicotinamide})_{6-n}]^{2+}$ [**25** ($n = 5$), **26** ($n = 4$, trans-), **27** ($n = 4$, cis-)] have been synthesized by reacting the nitrile cluster solvate with excess isonicotinamide (Scheme 6).[26] In the product, the substitutionally inert phosphine ligands serve to protect five, four, or four of the rhenium sites, respectively, while the amide ligand(s) occupy the remaining site(s) via Re−N(pyridyl) coordination. The amide function prefers paired amide−amide hydrogen-bonding interaction, while the specific cluster isomer determines geometry and dimensional extent of the resultant assembly.

The solid-state structures of the supramolecules were established crystallographically. The first of the series is the monoisonicotinamide complex **25** (Figure 9a). The isonicotinamide ligand is bound to the non-phosphine-protected Re site via the pyridyl nitrogen. Each cluster engages in self-complementary amide−amide hydrogen bonding to a cluster in a neighboring cell, generating a "zero-dimensional" hydrogen-bonded dimer. Using *trans*-$[Re_6(\mu_3\text{-}Se)_8(PEt_3)_4(\text{isonicotinamide})_2](SbF_6)_2$ (**26**), an infinite, one-dimensional chain featuring the cluster units and the cluster-linking hydrogen bonds results (Figure 9b). *cis*-$[Re_6(\mu_3\text{-}Se)_8(PEt_3)_4(\text{isonicotinamide})_2](SbF_6)_2$ (**27**) in the solid state also features one-dimensional chains of clusters, displaying a zigzag topology due to cis displacement of the isonicotinamide ligands (Figure 9c). The formation of a hydrogen-bonded square is not realized, probably due to the otherwise thermodynamically disfavored porous structure and packing thereof.

B. Multicluster Arrays Mediated by Secondary Metal Coordination. Cluster complexes possessing additional pyridyl N atoms are capable of further metal coordination. Such cluster complexes (**28** and **29**, Figure 10) can be

Scheme 6

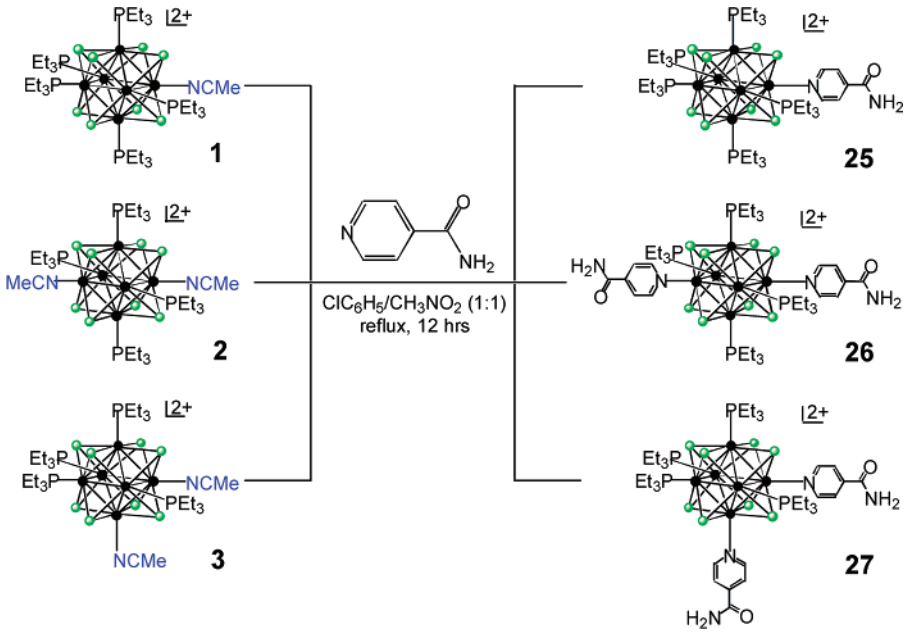

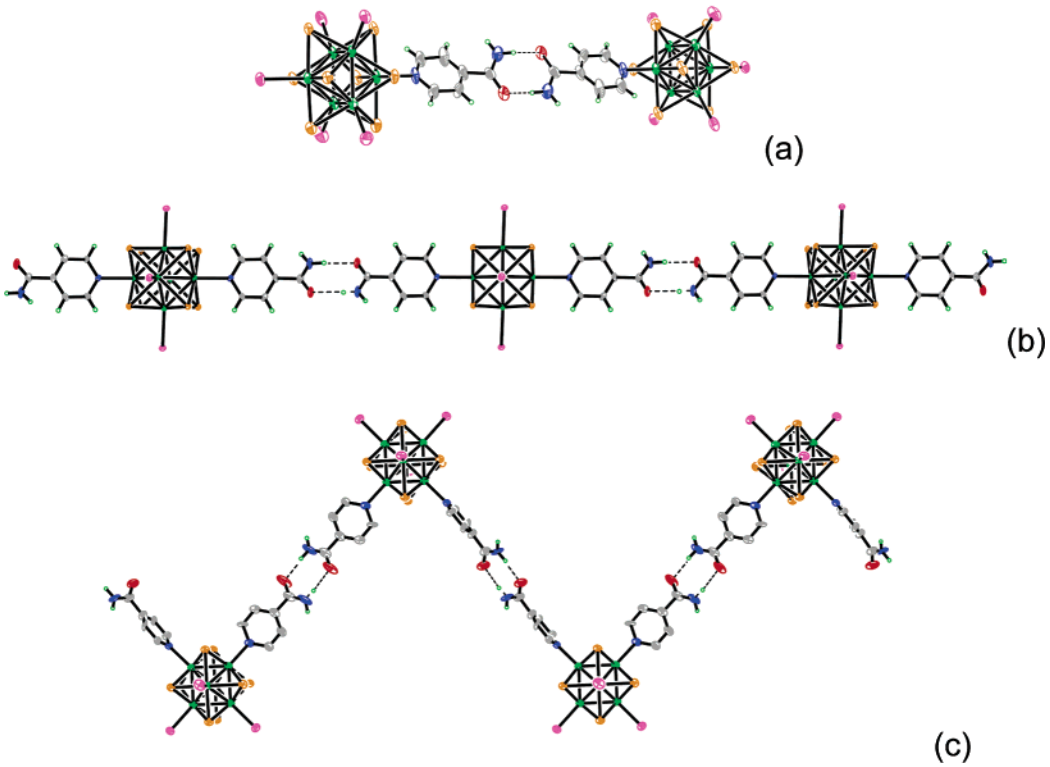

FIGURE 9. ORTEP views (50% ellipsoids) of three hydrogen-bonded arrays of the $[Re_6(\mu_3\text{-}Se)_8]^{2+}$ clusters [(a) **25**, (b) **26**, and (c) **27**]. Color scheme: C, gray; N, blue; O, red; P, purple; Re, green; Se, brown.

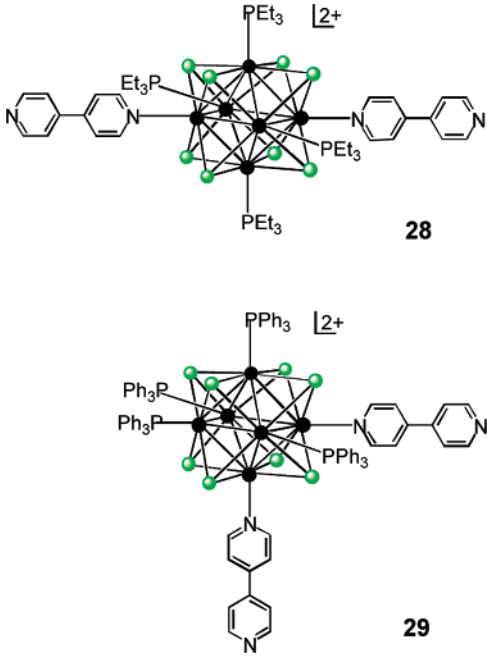

FIGURE 10. Molecular structures of two cluster complex-based ligands (**28**, **29**) site-differentiated with inert phosphine and metal-coordinating 4,4′-dipyridyl ligands.

readily prepared from the corresponding nitrile solvates and an excess of 4,4′-dipyridyl. If the structural possibilities due to the local coordination geometry of the secondary metal ions and the cluster ligand/metal ion ratio are considered, one may envision a great variety of cluster assemblies resulting from this crystal engineering approach.

Using *trans*-$[Re_6(\mu_3\text{-}Se)_8(PEt_3)_4(4,4'\text{-dipyridyl})_2](SbF_6)_2$ (**28**) as a cluster-expanded dipyridyl ligand for secondary coordination with Co^{2+}, the first polymeric cluster array mediated by the metal ions, $\{Co(NO_3)_3[Re_6(\mu_3\text{-}Se)_8(PEt_3)_4(4,4'\text{-dipyridyl})_2]\}(SbF_6)$ (**28**·Co^{2+}, Figure 11), was obtained.[27] It is a linear polymer with a repeat unit consisting of a single *trans*-$[Re_6(\mu_3\text{-}Se)_8(PEt_3)_4(4,4'\text{-dipyridyl})_2]$ unit bound to a Co^{2+} ion via the open nitrogen of a single 4,4′-dipyridyl ligand. The Co^{2+} is bound to a second pyridyl nitrogen from the next repeat unit, and the local $N_{pyridyl}$—Co^{2+}—$N_{pyridyl}$ coordination arrangement is trans. The polymer formed by this repeat unit has significant curvature between the Re atom coordinated to one end of the 4,4′-dipyridyl ligand and the Co^{2+} unit at the other. The curvature results in the polymers forming sinusoidal chains of modest amplitude. The chains have their cluster and Co^{2+} units shifted slightly with respect to one another, leading to alternating layers of opposing "phases" and the overall packing shown in Figure 11.

The sinusoidal shape of the chains observed in the Co^{2+}-mediating coordination polymer persists in its Cd^{2+} analogue $\{Cd(NO_3)_3[Re_6(\mu_3\text{-}Se)_8(PEt_3)_4(4,4'\text{-dipyridyl})_2]\}(SbF_6)$ (**28**·Cd^{2+}). However, the packing diagram is unique in this particular case in the manner that the chains interact within a given layer. Each adjacent chain is oriented with the cluster units and the Cd^{2+} units exactly parallel and in close contact. In this way the peaks and troughs of the neighboring sinusoidal chains meet and are held together by hydrophobic and hydrophilic interactions at the cluster and Cd^{2+} positions, respectively. The result of this unique packing mode is a large opening

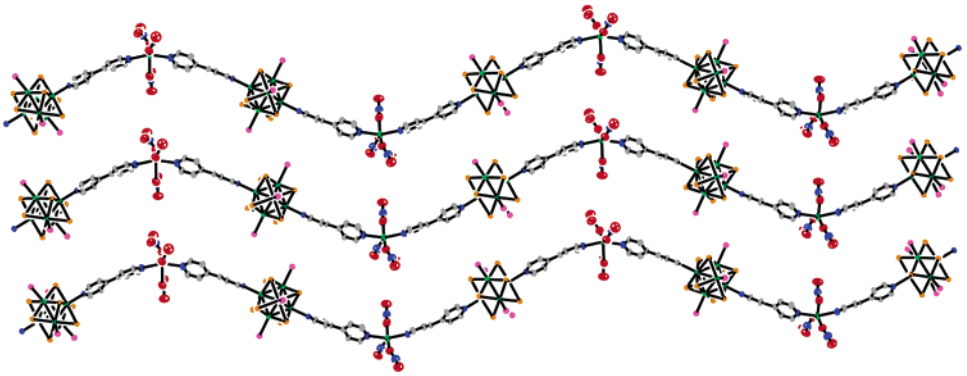

FIGURE 11. One layer of the Co^{2+}-mediated cluster assembly (**28**·Co^{2+}) shown with ethyl groups, hydrogen atoms, unbound counterions, and solvent omitted for clarity. Color scheme: C, gray; N, blue; O, red; P, purple; Re, green; Se, brown.

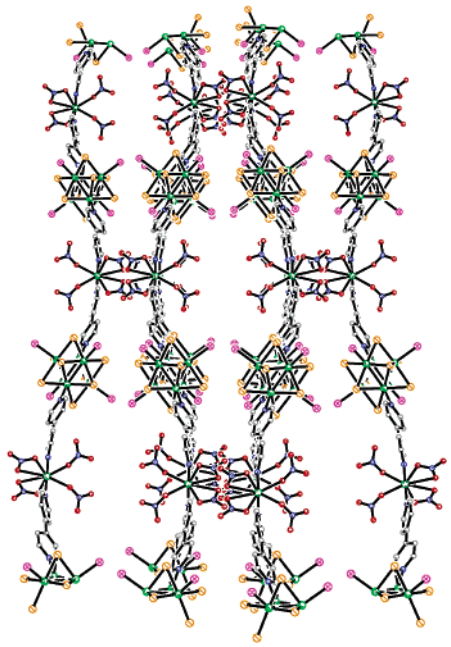

FIGURE 12. Ball-and-stick representation of the packing diagram of **28**·Cd^{2+}, the porous polymorph of the Cd^{2+}-mediated cluster assembly. Ethyl groups, solvent, and uncoordinated counterions are omitted for clarity. Color scheme: N, blue; O, red; P, purple; Re, green; Se, brown.

between sets of chains; this opening is clearly a large channel that runs in the *c* direction (Figure 12).

With Zn^{2+} as the secondary metal ion, the coordination polymer obtained, $\{Zn(NO_3)_3[Re_6(\mu_3\text{-}Se)_8(PEt_3)_4(4,4'\text{-dipyridyl})_2]\}(SbF_6)$ (**28**·Zn^{2+}), is chemically very similar to those of Co^{2+} and Cd^{2+}, but structurally distinct. The repeat unit is essentially the same as the previous two cases except that the $N_{pyridyl}-Zn^{2+}-N_{pyridyl}$ coordination mode is cis with respect to Zn^{2+}, with an average $N_{pyridyl}-Zn^{2+}-N_{pyridyl}$ angle of 88°. The effect of this coordination mode is to afford overall one-dimensional zigzag polymer chains (Figure 13a), rather than the sinusoidal polymers. As in the previous two structures, the zigzag polymers form layers of parallel chains, but the layers are interpenetrated (Figure 13b). In the spaces between chains in a given sheet, chains forming the penetrating layer run roughly normal to the plane of the sheet. This packing mode results in the formation of small channels that pass through the crystal in the *b* direction between neighboring Zn^{2+} sites.

Although intriguing, the porous materials prepared with the linear cluster ligands are serendipitous. To prepare rationally designed porous materials, we have resorted to the nonlinear building blocks to direct the self-assembly process. This approach has been successful but provided some surprising results as well.

In an attempt to prepare porous, square-shaped complexes utilizing the cluster-as-ligand approach, we have studied the coordination of *cis*-$[Re_6(\mu_3\text{-}Se)_8(PPh_3)_4(4,4'\text{-dipyridyl})_2](SbF_6)_2$ (**29**) with $Cd(NO_3)_2$.[28] The cluster building block of interest was prepared by reacting *cis*-$[Re_6(\mu_3\text{-}Se)_8(PPh_3)_4(CH_3CN)_2](SbF_6)_2$ with an excess of 4,4′-dipyridyl. There is an enforced right angle between the two dipyridyl ligands, each with one of its N atoms coordinated to the cluster, leaving the other available for further metal coordination. A 1:1 (molar) mixture of **29** in CH_2Cl_2 and $Cd(NO_3)_2$ in methanol was subjected to ether diffusion, resulting in thick plate-shaped crystals. Crystallographic analysis revealed that this compound, formulated as $[\{Re_6(\mu_3\text{-}Se)_8(PPh_3)_4(4,4'\text{-dipyridyl})_2\}_2\{Cd(NO_3)_2\}](SbF_6)_4\cdot 21C_4H_{10}O\cdot 21CH_2Cl_2$ (**30**), forms a one-dimensional chain of corner-sharing squares (Figure 14, left) in the solid state. Each shared corner is a single octahedrally coordinated Cd^{2+} ion, bound in the equatorial plane by four pyridyl nitrogens and axially by two η^1-NO_3^- ligands. The unshared corners are formed by the $[Re_6(\mu_3\text{-}Se)_8]^{2+}$ clusters.

Perhaps most interesting, however, is the observed cluster/Cd^{2+} ratio. Although pains were taken to ensure a 1:1 ratio, the structure exhibits a 2:1 cluster/Cd^{2+} ratio. Because of this unexpected result, we have sought to probe what effects, if any, the cluster/Cd^{2+} ratio had on the final outcome by reacting **29** with a large excess of the Cd^{2+} salt. Compound **30**, formulated as $[\{Re_6(\mu_3\text{-}Se)_8(PPh_3)_4(4,4'\text{-dipyridyl})_2\}\{Cd(NO_3)_3\}](NO_3)\cdot 2C_4H_{10}O\cdot CH_2Cl_2$ (**31**), was isolated quantitatively. Its solid-state structure (Figure 14, right) is a one-dimensional zigzag chain, featuring repeating units of $\{[Re_6(\mu_3\text{-}Se)_8(PPh_3)_4(4,4'\text{-dipyridyl})_2][Cd(NO_3)_3]\}^-$. As with compound **30**, the chains clearly reflect the geometric constraint imposed by the cluster ligands but also show flexibility at the Cd^{2+} site.

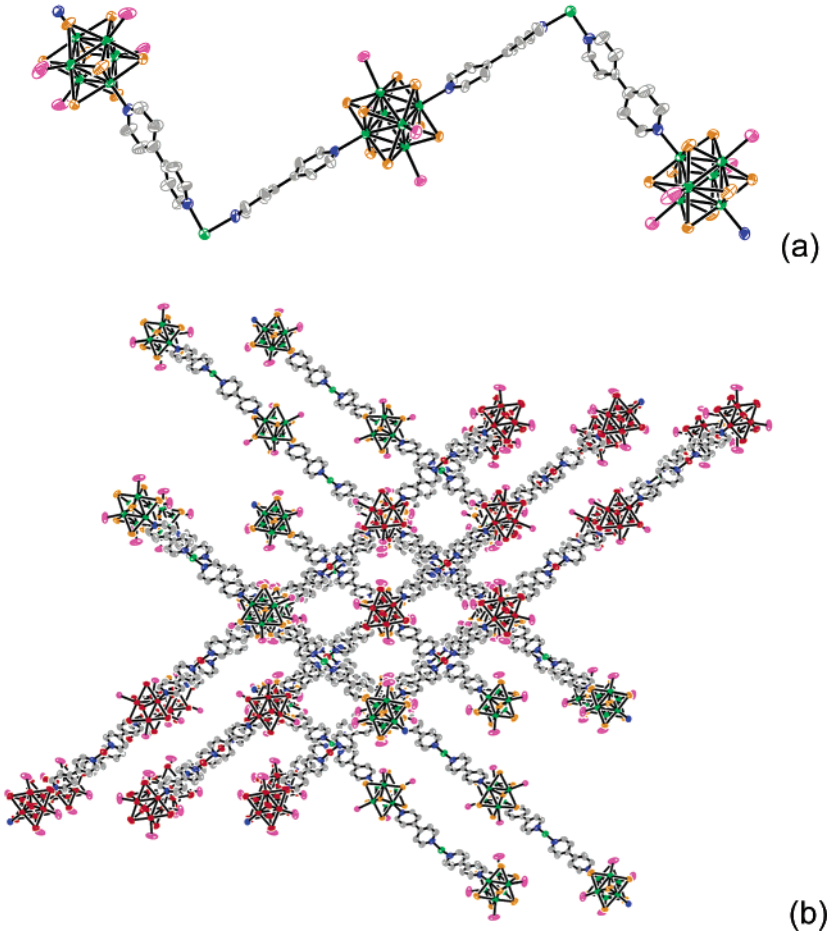

FIGURE 13. (a) Single chain of the Zn^{2+}-mediated cluster assembly (**28**·Zn^{2+}). Ethyl groups, protons, counterions, and solvent are omitted for clarity. (b) Packing diagram of the Zn^{2+} structure viewed down the *b* axis. The clusters in the two interpenetrating layers are shown in red and green, respectively.

The chain structure of **31** is formally derived from **30** by replacing the cluster on one side of the squares with a nitrato ligand. Indeed, as confirmed by crystallographic determination of cell parameters, complex **31** is isolated from the reaction of complex **30** with an excess of $Cd(NO_3)_2$ in a methanolic solution upon ether vapor diffusion. The formation of a particular polymeric structure may be rationalized in terms of two competing thermodynamic forces—optimization of crystal density/close packing of the multicluster arrays and maximization of Cd^{2+} pyridyl coordination. It follows that the fused square represents a compromise between optimal Cd^{2+} coordination and structural density and is the favored structure when the concentration of the cluster complex and that of the Cd^{2+} salt are comparable. In the presence of excess Cd^{2+}, however, the balance shifts to favor close packing, affording the zigzag chain that still exhibits the same skeletal arrangement of Cd^{2+} and cluster ligands.

V. Summary and Outlook

In this Account, we summarized our recent work in molecular and supramolecular constructions utilizing stereospecific hexanuclear rhenium selenide cluster building blocks. The cluster's versatility in this role is manifested in the variety of beautiful architectures and physically intriguing properties demonstrated, as well as the facile change of synthetic paradigms necessary to achieve these results.

The foundation of the cluster building blocks' versatility in application is the uniquely favorable synthetic chemistry of the cluster core itself. The cluster core's relative inertness prohibits stereochemical scrambling, ensuring a fixed geometry for a given isomer. In effect, the cluster complex is a rigid building block with defined geometry that limits the structural possibilities of a multicluster array upon assembly. In each of the examples presented here, the geometry of the cluster is indeed faithfully expressed in the solid state. The chemistry described in the second part of this Account appears to be especially versatile, as the self-assembly process is also dependent on the hydrogen bond-forming functionality and coordination geometry of the secondary metal ions, which eventually dictate the overall architectures of the resulting extended systems. The combined effect of the cluster's geometric directing power and the reasonable degree of predictability of hydrogen bonding and metal–ligand coordination interactions points to the possibility of generating other novel cluster-supported architectures and possibly molecularly engineered materials.

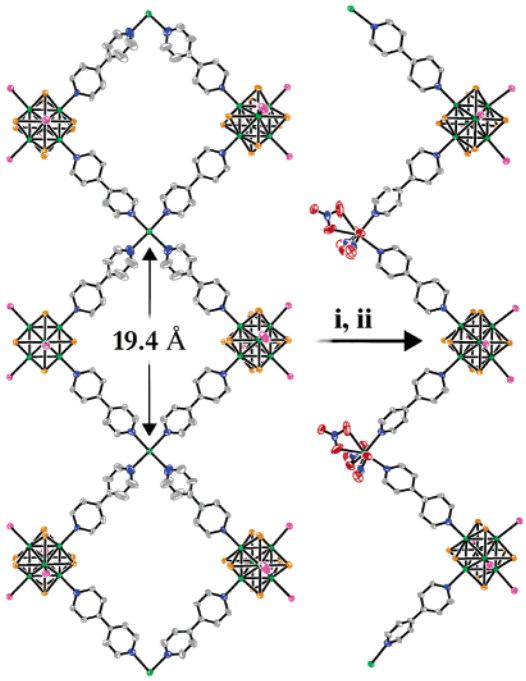

FIGURE 14. Thermal ellipsoid plots of **30** (left) and **31** (right) rendered at 50% probability. Only the framework structure is shown. Conversion in two steps: (i) $Cd(NO_3)_2/CH_3OH$; (ii) ether diffusion. Color scheme: C, gray; N, blue; O, red; P, purple; Re, green; Se, brown.

Although we have explored a range of structural types and their synthetic methods, often with interesting and unexpected results, we are only at the beginning of a very exciting journey. With continuing efforts from our group and others, we anticipate many new discoveries that incorporate these clusters into discrete or more extended systems and further advancement of the chemistry of the $[Re_6(\mu_3\text{-}Se)_8]^{2+}$ clusters in general.

We acknowledge the support of Research Corporation and the Donors of the Petroleum Research Fund. H.D.S. has been the recipient of a GenCorp Fellowship for Synthetic Chemistry. The CCD-based X-ray diffractometer was purchased through NSF Grant No. CHE-96103474.

References

(1) Merkle, R. C. Molecular Building Blocks and Development Strategies for Molecular Nanotechnology. *Nanotechnology* **2000**, *11*, 89−99.
(2) For selected reviews, see: (a) Evans, O. W.; Lin, W. Crystal Engineering of NLO Materials Based on Metal-Organic Coordination Networks. *Acc. Chem. Res.* **2002**, *35*, 511−522. (b) Leininger, S.; Olenyuk, B.; Stang, P. J. Self-Assembly of Discrete Cyclic Nanostructures Mediated by Transition Metals. *Chem. Rev.* **2000**, *100*, 853−908. (c) Caulder, D. N.; Raymond, K. N. The Rational Design of High-Symmetry Coordination Clusters. *J. Chem. Soc., Dalton Trans.* **1999**, 1185−1200. (d) Yaghi, O. M.; Li, H.; Davis, C.; Richardson, D.; Groy, T. L. Synthetic Strategies, Structure Patterns, and Emerging Properties in the Chemistry of Modular Porous Solids. *Acc. Chem. Res.* **1998**, *31*, 474−484.
(3) *Metal Clusters in Chemistry*; Braunstein, P., Oro, L. A., Raithby, P. R., Eds.; Wiley-VCH: New York, 1999.
(4) Rosi, N. L.; Eckert, J.; Eddaoudi, M.; Vodak, D. T.; Kim, J.; O'Keeffe, M.; Yaghi, O. M. Hydrogen Storage in Microporous Metal-Organic Frameworks. *Science* **2003**, *300*, 1127−1129.
(5) Seo, J. S.; Whang, D.; Lee, H.; Jun, S. I.; Oh, J.; Jeon, Y. J.; Kim, K. A Homochiral Metal−Organic Porous Material for Enantioselective Separation and Catalysis. *Nature* **2000**, *404*, 982−986.
(6) Cotton, F. A.; Lin, C.; Murillo, C. A. Supramolecular Arrays Based on Dimetal Building Units. *Acc. Chem. Res.* **2001**, *34*, 759−771.
(7) Bain, R. L.; Shriver, D. F.; Ellis, D. E. Extended Materials Based on the $[Mo_6Cl_8]^{4+}$ Building Block Bridged by 4,4′-Bipyridine. *Inorg. Chim. Acta* **2001**, *325*, 171−174.
(8) Jin, S.; DiSalvo, F. J. 3-D Coordination Network Structures Constructed from $[W_6S_8(CN)_6]^{6-}$ Anions. *Chem. Mater.* **2002**, *14*, 3448−3457.
(9) Disalvo, F. J. Some Remarkable Properties of Transition Metal Chalcogenide Compounds. *Ann. Chim.* **1982**, *7*, 109−118.
(10) Gabriel, J. C. P.; Boubekeur, K.; Uriel, S.; Batail, P. Chemistry of Hexanuclear Rhenium Chalcohalide Clusters. *Chem. Rev.* **2001**, *101*, 2037−2066.
(11) Long, J. R.; McCarty, L. S.; Holm, R. H. A Solid State Route to Molecular Clusters: Access to the Solution Chemistry of $[Re_6Q_8]^{2+}$ (Q = S, Se) Core-Containing Clusters via Dimensional Reduction. *J. Am. Chem. Soc.* **1996**, *118*, 4603−4616.
(12) Prokopuk, N.; Shriver, D. F. The Octahedral M_6Y_8 and M_6Y_{12} Clusters of Group 5 and 6 Transition Metals. *Adv. Inorg. Chem.* **1998**, *46*, 1−49.
(13) (a) Zheng, Z.; Long, J. R.; Holm, R. H. A Basis Set of Re_6Se_8 Cluster Building Blocks and Demonstration of Their Linking Capability: Directed Synthesis of an $Re_{12}Se_{16}$ Dicluster. *J. Am. Chem. Soc.* **1997**, *119*, 2163−2171. (b) Zheng, Z.; Holm, R. H. Cluster Condensation by Thermolysis: Synthesis of a Rhomb-Linked $Re_{12}Se_{16}$ Dicluster and Factors Relevant to the Formation of the $Re_{24}Se_{32}$ Tetracluster. *Inorg, Chem.* **1997**, *36*, 5173−5178. (c) Zheng, Z.; Gray, T.; Holm, R. H. Synthesis and Structures of Solvated Monoclusters and Bridged Di- and Triclusters Based on the Cubic Building Block $[Re_6(\mu_3\text{−}Se)_8]^{2+}$. *Inorg. Chem.* **1999**, *38*, 4888−4895. (d) Willer, M. W.; Long, J. R.; McLauchlan, C. C.; Holm, R. H. Ligand Substitution Reactions of $[Re_6S_8Br_6]^{4-}$: A Basis Set of Re_6S_8 Clusters for Building Multicluster Assemblies. *Inorg. Chem.* **1998**, *37*, 328−333. (e) Gray, T. G.; Holm, R. H. Site-Differentiated Hexanuclear Rhenium(III) Cyanide Clusters $[Re_6Se_8(PEt_3)_n(CN)_{6-n}]^{n-4}$ (n = 4, 5) and Kinetics of Solvate Ligand Exchange on the Cubic $[Re_6Se_8]^{2+}$ Core. *Inorg. Chem.* **2002**, *41*, 4211−4216.
(14) (a) Chen, Z.-N.; Yoshimura, T.; Abe, M.; Sasaki, Y.; Ishizaka, S.; Kim, H.-B.; Kitamura, N. Chelate Formation around a Hexarhenium Cluster Core by the Diphosphane Ligand $Ph_2P(CH_2)_6PPh_2$. *Angew. Chem., Int. Ed.* **2001**, *40*, 239−242. (b) Gray, T. G.; Rudzinski, C. M.; Meyer, E. E.; Holm, R. H.; Nocera, D. G. Spectroscopic and Photophysical Properties of Hexanuclear Rhenium(III) Chalcogenide Clusters. *J. Am. Chem. Soc.* **2003**, *125*, 4755−4770. (c) Arratia-Pérez, R.; Hernández-Acevedo, L. The $Re_6Se_8Cl_6^{4-}$ and $Re_6Se_8I_6^{4-}$ Cluster Ions: Another Example of Luminescent Clusters? *J. Chem. Phys.* **1999**, *111*, 168−172.
(15) Köhler, A.; Wilson, J. S.; Friend, R. H. Fluorescence and Phosphorescence in Organic Materials. *Adv. Mater.* **2002**, *14*, 701−707.
(16) (a) Bennett, M. V.; Beauvais, L. G.; Shores, M. P.; Long, J. R. Expanded Prussian Blue Analogues Incorporating $[Re_6Se_8(CN)_6]^{3-/4-}$ Clusters: Adjusting Porosity via Charge Balance. *J. Am. Chem. Soc.* **2001**, *123*, 8022−8032. (b) Beauvais, L. G.; Shores, M. P.; Long, J. R. Cyano-Bridged Re_6Q_8 (Q = S, Se) Cluster−Cobalt(II) Framework Materials: Versatile Solid Chemical Sensors. *J. Am. Chem. Soc.* **2000**, *122*, 2763−2772.
(17) Naumov, N. G.; Virovets, A. V.; Sokolov, N. S.; Artemkina, S. B.; Fedorov, V. E. A Novel Framework Type for Inorganic Clusters with Cyanide Ligands: Crystal Structures of $Cs_2Mn_3[Re_6Se_8(CN)_6]_2\cdot 15H_2O$ and $(H_3O)_2Co_3[Re_6Se_8(CN)_6]_2\cdot 14.5H_2O$. *Angew. Chem., Int. Ed.* **1998**, *37*, 1943−1945.
(18) Selby, H. D.; Zheng, Z.; Gray, T. G.; Holm, R. H. Bridged Multiclusters Derived from the Face-Capped Octahedral $[Re_6Se_8]^{2+}$ Cluster Core. *Inorg. Chim. Acta* **2001**, *312*, 205−208.
(19) Roland, B. K.; Selby, H. D.; Carducci, M. D.; Zheng, Z. Built to Order: Molecular Tinkertoys from the $[Re_6(\mu_3\text{-}Se)_8]^{2+}$ Clusters. *J. Am. Chem. Soc.* **2002**, *124*, 3222−3223.
(20) (a) Wang, R.; Zheng, Z. Dendrimers Supported by the $[Re_6Se_8]^{2+}$ Metal Cluster Core. *J. Am. Chem. Soc.* **1999**, *121*, 3549−3550. (b) Roland, B. K.; Carter, C.; Zheng, Z. Routes to Metallodendrimers of the $[Re_6(\mu_3\text{-}Se)_8]^{2+}$ Core-Containing Clusters. *J. Am. Chem. Soc.* **2002**, *124*, 6234−6235.
(21) Roland, B. K.; Selby, H. D.; Zheng, Z. Unpublished results.
(22) Thalladi, V. R.; Brasselet, S.; Weiss, H.-C.; Bläser, D.; Katz, A. K.; Carrell, H. L.; Boese, R.; Zyss, J.; Nangia, A.; Desiraju, G. R. Crystal Engineering of Some 2,4,6-Triaryloxy-1,3,5-Triazines: Octupolar Nonlinear Materials. *J. Am. Chem. Soc.* **1998**, *120*, 563−2577.
(23) Anson, F. C.; Shi, C. N.; Steiger, B. Novel Multinuclear Catalysts for the Electroreduction of Dioxygen Directly to Water. *Acc. Chem. Res.* **1997**, *30*, 437−444.

(24) Balzani, V.; Campagna, S.; Denti, G.; Juris, A.; Serroni, S.; Venturi, M. Designing Dendrimers Based on Transition-Metal Complexes. Light-Harvesting Properties and Predetermined Redox Patterns. *Acc. Chem. Res.* **1998**, *31*, 26−34.
(25) Denti, G.; Serroni, S.; Campagna, S.; Juris, A.; Ciano, M.; Balzani, V. In *Perspectives in Coordination Chemistry*; Williams, A. F., Floriani, C., Merbach, A. E., Eds.; VCH: New York, 1992.
(26) Selby, H. D.; Roland, B. K.; Carducci, M. D.; Zheng, Z. Hydrogen-Bonded Extended Arrays of the $[Re_6(\mu_3\text{-}Se)_8]^{2+}$ Core-Containing Clusters. *Inorg. Chem.* **2003**, *42*, 1656−1662.
(27) Selby, H. D.; Orto, P.; Zheng, Z. A Modular Crystal Engineering Approach to Coordination Polymers Supported by the Face-Capped $[Re_6(\mu_3\text{-}Se)_8]^{2+}$ Clusters. *Polyhedron* **2003**, *22*, 2999−3008.
(28) Selby, H. D.; Orto, P.; Carducci, M. D.; Zheng, Z. Novel Concentration Driven Structural Interconversion in Shape-Specific Solids Supported by the Octahedral $[Re_6(\mu_3\text{-}Se)_8]^{2+}$ Cluster Core. *Inorg. Chem.* **2002**, *41*, 6175−6177.

AR020134C